



Reversible switching and stability of the epigenetic memory system in bacteria

Dimitri Graf¹, Laura Laistner¹, Viviane Klingel², Nicole E. Radde² , Sara Weirich¹ and Albert Jeltsch¹ 

¹ Institute of Biochemistry and Technical Biochemistry, University of Stuttgart, Germany

² Institute for Systems Theory and Automatic Control, University of Stuttgart, Germany

Keywords

DNA methylation; epigenetic memory system; gene regulation; mathematical modelling; zinc finger

Correspondence

A. Jeltsch, Institute of Biochemistry and Technical Biochemistry, University of Stuttgart, Allmandring 31, 70569 Stuttgart, Germany

Tel: +49 711 685 64390

E-mail: albert.jeltsch@ibtb.uni-stuttgart.de

(Received 28 August 2022, revised 22 October 2022, accepted 22 November 2022)

doi:10.1111/febs.16690

In previous work, we have developed a DNA methylation-based epigenetic memory system that operates in *Escherichia coli* to detect environmental signals, trigger a phenotypic switch of the cells and store the information in DNA methylation. The system is based on the CcrM DNA methyltransferase and a synthetic zinc finger (ZnF4), which binds DNA in a CcrM methylation-dependent manner and functions as a repressor for a *ccrM* gene expressed together with an *egfp* reporter gene. Here, we developed a reversible reset for this memory system by adding an increased concentration of ZnSO₄ to the bacterial cultivation medium and demonstrate that one bacterial culture could be reversibly switched ON and OFF in several cycles. We show that a previously developed differential equation model of the memory system can also describe the new data. Then, we studied the long-term stability of the ON-state of the system over approximately 100 cell divisions showing a gradual loss of ON-state signal starting after 4 days of cultivation that is caused by individual cells switching from an ON- into the OFF-state. Over time, the methylation of the ZnF4-binding sites is not fully maintained leading to an increased OFF switching probability of cells, because stronger binding of ZnF4 to partially demethylated operator sites leads to further reductions in the cellular concentrations of CcrM. These data will support future design to further stabilize the ON-state and enforce the binary switching behaviour of the system. Together with the development of a reversible OFF switch, our new findings strongly increase the capabilities of bacterial epigenetic biosensors.

Introduction

One emerging field of synthetic biology is the design of artificial genetic and epigenetic signalling networks, which are able to detect, process and store information about external signals in bacterial, mammalian and plant cells [1–5]. Synthetic genetic circuits have been developed and widely applied to understand regulatory functions and modulate signalling outcomes [6]. Gene circuits allow for two types of basic functionalities: In a sensor system, the acute presence of a signal leads to

a cellular response, while a memory system stores information about the past occurrence of a signal over long time periods, even after the decline in the signal. Ideally, a sensor system provides both types of readout allowing to discriminate between an acute presence of the signal and past exposure. On the one hand, memory systems require stable ON- and OFF-states of binary switches, but, on the other hand, an easy way of reversible switching between these states is desirable

Abbreviations

CcrM, *Caulobacter crescentus* cell-cycle-regulated methyltransferase; ZnF, synthetic zinc finger protein; ZnF4, homotetramer of the ZnF protein.

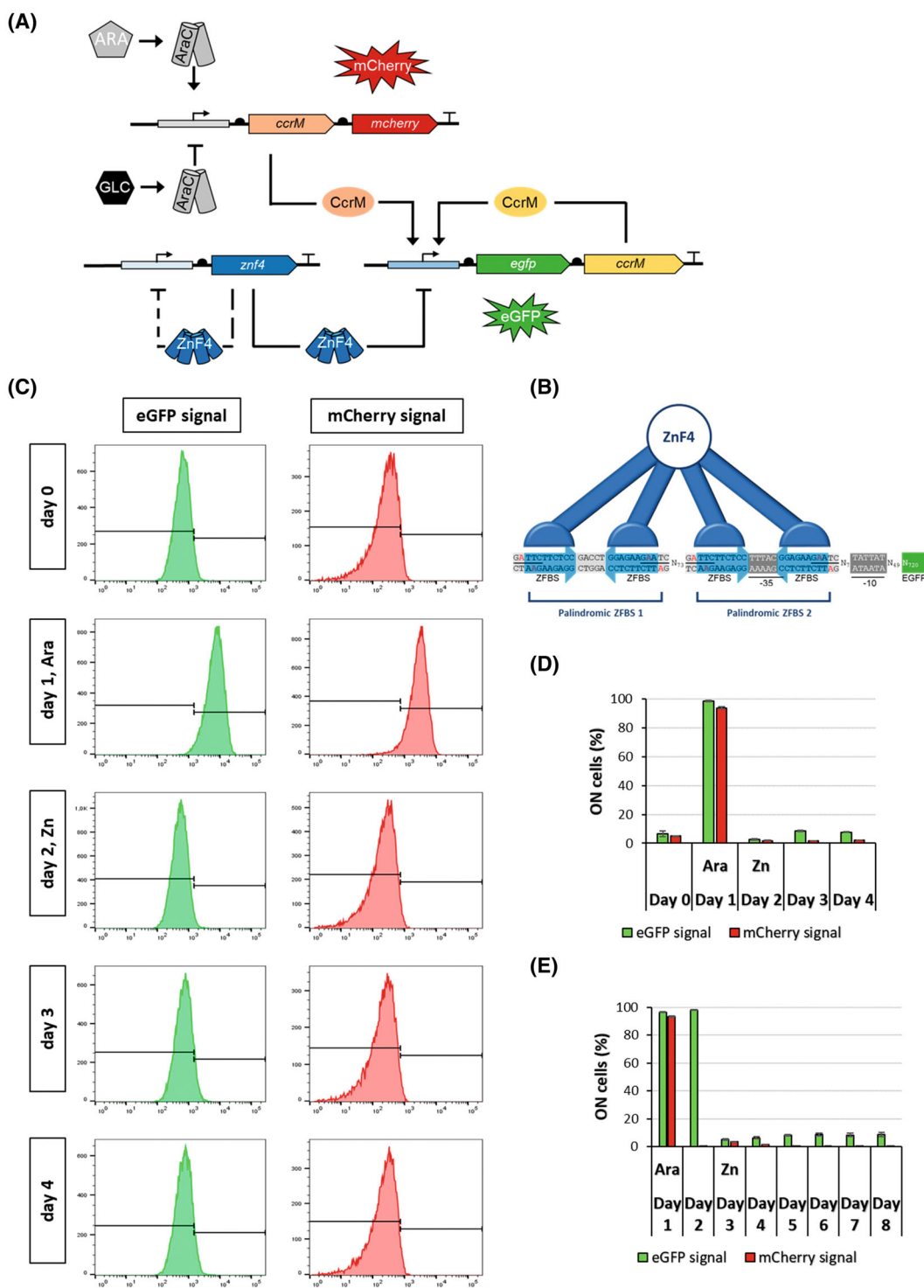
for many applicative purposes. These opposing demands can be provided by epigenetic systems, because by definition, epigenetic signals can be stably propagated in cells, although they are still reversible as no genetic changes occur [7]. This makes them particularly suitable for a potential sensor that could store information in a memory system but could be reset at any time during the experiment or application.

DNA methylation is a key epigenetic signal in bacteria and higher organisms [8–11]. In the past, different artificial DNA methylation-based epigenetic gene expression switches were developed in bacteria and mammalian cells that employ two well-studied bacterial DNA-(adenine N6)-methyltransferases, the *Escherichia coli* deoxyadenosine DNA methyltransferase (Dam) and the *Caulobacter crescentus* cell-cycle-regulated methyltransferase (CcrM) [12–15]. Using CcrM, we have developed a set of DNA methylation-based epigenetic memory systems in *E. coli* [12,15] that are able to detect nutrients like L-arabinose, environmental cues like tetracycline as an example of a toxin and also physical stimuli like heat or UV radiation. These DNA methylation-based memory systems (Fig. 1A) employ a designed synthetic zinc finger protein (ZnF), which binds to a GGAGAAGAA sequence, if the underlined adenosine residue does not carry N6 methylation [12,16]. If this sequence is combined with a CcrM GANTC recognition site in a GGAGAAGAATC sequence, ZnF binding is controlled by CcrM methylation. In the memory system, ZnF is used as a repressor for a *ccrM* gene, which is expressed together with an *egfp* reporter gene in a polycistronic operon. The ZnF repressor protein binds cooperatively as a homotetramer (ZnF4) to a pair of palindromic binding sites in the artificial *ccrM* promoter in a CcrM methylation-sensitive manner as described above (Fig. 1B). Initially, the ZnF4-binding sites are unmethylated, allowing ZnF4 binding and

leading to the repression of CcrM and eGFP expression (OFF-state of the memory system). To activate the system, a second plasmid is used which contains a second copy of the *ccrM* gene (trigger CcrM) under the control of a promoter that is regulated by an external signal of interest. The application of the external signal causes the expression of the trigger *ccrM* gene, together with an mCherry fluorophore. The trigger CcrM then methylates the ZnF4-binding sites on the memory plasmid leading to the dissociation of the ZnF4 repressor and expression of the memory plasmid CcrM, which establishes a positive feedback loop (ON-state of the system). This ON-state is maintained by the activity of the memory CcrM, even if the trigger signal has disappeared. It can be detected by the eGFP fluorescence while mCherry fluorescence is transient, indicating the acute presence of the trigger signal. Resetting of the system was implemented before by including additional degradation tags and regulated proteases [12], but this approach was inconvenient and not suitable for many applications. Moreover, simulations and experimental data showed that the stability of the ON-state of this system is not perfect [12,15,17], which also limits the application of the system.

In this work, we have investigated the spontaneous and enforced switching of the memory system from the ON- into the OFF-state. Firstly, we developed a simple and reversible system reset by adding an increased concentration of ZnSO₄ to the cultivation medium of the *E. coli* cells. Using this, we demonstrate that one bacterial culture could be reversibly switched ON and OFF in several cycles. Secondly, we show that a previously developed differential equation model of the memory system [17] can describe the new data. Thirdly, we studied the long-term stability of the ON-state of the system over approximately 100 cell divisions and analysed the fraction of cells in ON- and OFF-state showing that loss of ON-state signal is caused by individual

Fig. 1. Scheme of the DNA methylation-based memory system and establishment of an OFF switch. (A) Scheme of the DNA methylation-based memory system (modified from Maier et al.) [12]. For details, refer to the text. (B) Scheme of the promoter region of the memory operon (light blue box in panel A). The tetrameric ZnF4 binds to two pairs of palindromic zinc finger-binding sites (ZFBs). GANT sites are indicated by a black line. Adenine residues that are methylated by CcrM are coloured red. Relevant genetic elements are annotated. (C) Exemplary flow cytometry histograms showing the OFF switch of cultures by increasing the ZnSO₄ concentration in the growth medium. The figure shows histograms of eGFP (green) and mCherry (red) fluorescence signals of the memory and trigger systems collected over 4 days. The horizontal axis shows the fluorescence signal in log scale and the vertical axis indicates the number of cells in the distribution. The corresponding gates to distinguish ON- and OFF-state cells are indicated (see also Fig. S1). (D) Fraction of cells in the ON-state during the OFF switch is shown in panel C. (E) Long-term cultivation experiment showing that the OFF-state is stable for several days. Panels D and E show the fraction of cells in ON-state for the eGFP (green) and mCherry (red) fluorescence signal. ON and OFF switching was induced by the addition of arabinose (0.02%, w/v) (indicated by “Ara”) and ZnSO₄ (300 μM, indicated by “Zn”) to the growth medium. Panels D and E show averages of three independent experiments. The error bar displays the SEM. Primary flow cytometry histograms for panel E are shown in Fig. S2.



cells switching back from the ON- into the OFF-state, not by a population drift. We show that over time, the methylation of the ZnF4-binding sites is not fully maintained leading to an increase in the probability of

a cell switching from the ON back into the OFF-state. These data will support future design to further stabilize the ON-state and enforce the binary switching behaviour of the system. This and the reversible

reprogramming of the memory device with the help of the OFF-switch strongly increases the capabilities of bacterial epigenetic biosensors.

Results

As described above, a DNA methylation-based memory switch system was established that responds to an arabinose trigger by a switch into an ON-state leading to eGFP expression [12]. However, in the available versions of the memory system, OFF switching could only be achieved by a second independent signalling system, which regulated proteolysis of CcrM [12]. This approach, although feasible, did not allow for easy and reversible switching of the system between ON- and OFF-states. However, a convenient OFF switch that does not interfere with other properties of the system is an important applicative property, to allow a system reset in OFF-state and calibration at the beginning of a signal recording period. Hence, it was one aim of this work to develop a new mechanism for switching the memory system into the OFF-state that ideally should be based on a small molecule repressor that can be added to the growth medium and does not require additional components inside the host bacterium.

Development of an OFF-switch procedure and reversible switching of the memory system

It is well known that efficient expression and folding of zinc-containing proteins in bacteria requires elevated Zn^{2+} concentrations in the growth media to provide sufficient Zn^{2+} inside the bacterial cells [18]. This effect is due to the central structural role of Zn^{2+} ions in folding of many zinc-containing proteins. The addition of $ZnSO_4$ to the growth medium was also an essential optimization parameter of the memory system in the past to achieve a stable OFF-state [12]. We hypothesized that further increasing the $ZnSO_4$ concentration in the bacterial growth medium (beyond the regularly applied $10\ \mu M$ $ZnSO_4$) would strengthen the DNA binding of ZnF4 due to its improved folding and stability. Therefore, we tested if treatment of cells containing the memory system with elevated concentration of $ZnSO_4$ could cause an OFF switch of the system. After systematic investigations, we found by flow cytometry readout of the system state that the addition of $300\ \mu M$ $ZnSO_4$ to the medium for 1 day caused robust OFF switching (Fig. 1C,D; Fig. S1). Long-term cultivation of the cells indicated that the OFF-state was stable for at least 5 days (Fig. 1E; Fig. S2).

Next, we wondered whether the treatment with elevated $ZnSO_4$ concentrations would affect the triggering of the system by arabinose and the long-term stability

of the ON-state. To investigate this, different bacterial cultures were continuously cultivated and the state of the memory system was evaluated each day by flow cytometry (Fig. 2). In alternating cycles, the cultures were treated with arabinose, or high concentrations of $ZnSO_4$ were added to the cultivation media, revealing that reversible switching between stable ON- and OFF-states could be achieved by the alternative treatment with the small molecule compounds finally allowing to realize ON–OFF–ON and ON–OFF–ON–OFF switching cycles (Fig. 2A,B; Figs S3 and S4). This finding indicates that the previous triggering of the system by arabinose or $ZnSO_4$ did not affect the ability for future changes of the system state. Our data illustrate that bacterial cultures could be reversibly switched between the ON- and OFF-states in several cycles and by this, a reversible memory device was developed.

Modelling of the OFF switch and flexible switching

Previously, we developed and validated a differential equation model to describe the different types of methylation-based epigenetic memory systems [17]. The mathematical model was shown to capture the switching dynamics of methylation levels and methyltransferase amounts induced by different inputs [17] and the same model could also be used to explore the conditions of system oscillations [19]. A detailed analysis showed that the system operates in the bistable range, but it is not robust to changes in parameters [17]. In particular, the system behaviour was shown to critically depend on the cell division rate. Allowing a moderate variability in the cell division rate between cells in a population, the model predicted a largely heterogeneous response of this population upon stimulation, in which more and more cells switched from the ON- to OFF-state over time, causing a slow drift of the population towards the OFF-state. To include the option of an OFF switch by addition of $ZnSO_4$, we increased the association rate of ZnF4 binding to the DNA (parameter a_1 in the model). This parameter comprises both the concentration of ZnF4, and its association rate constant to ZnF4-binding sites. The new experimental OFF-switch data (Figs 1E and 2A,B) were well described by increasing ZnF4 association by a factor of 1.3 under conditions of elevated $ZnSO_4$ instead of 1.0 under standard cultivation conditions (Fig. 3A–C). These results demonstrate that the previously defined model can fully capture also the new data. Moreover, a relatively small increase of about 30% of the binding of ZnF4 to its target sites can explain the efficient OFF switch of the memory system observed under our experimental conditions.

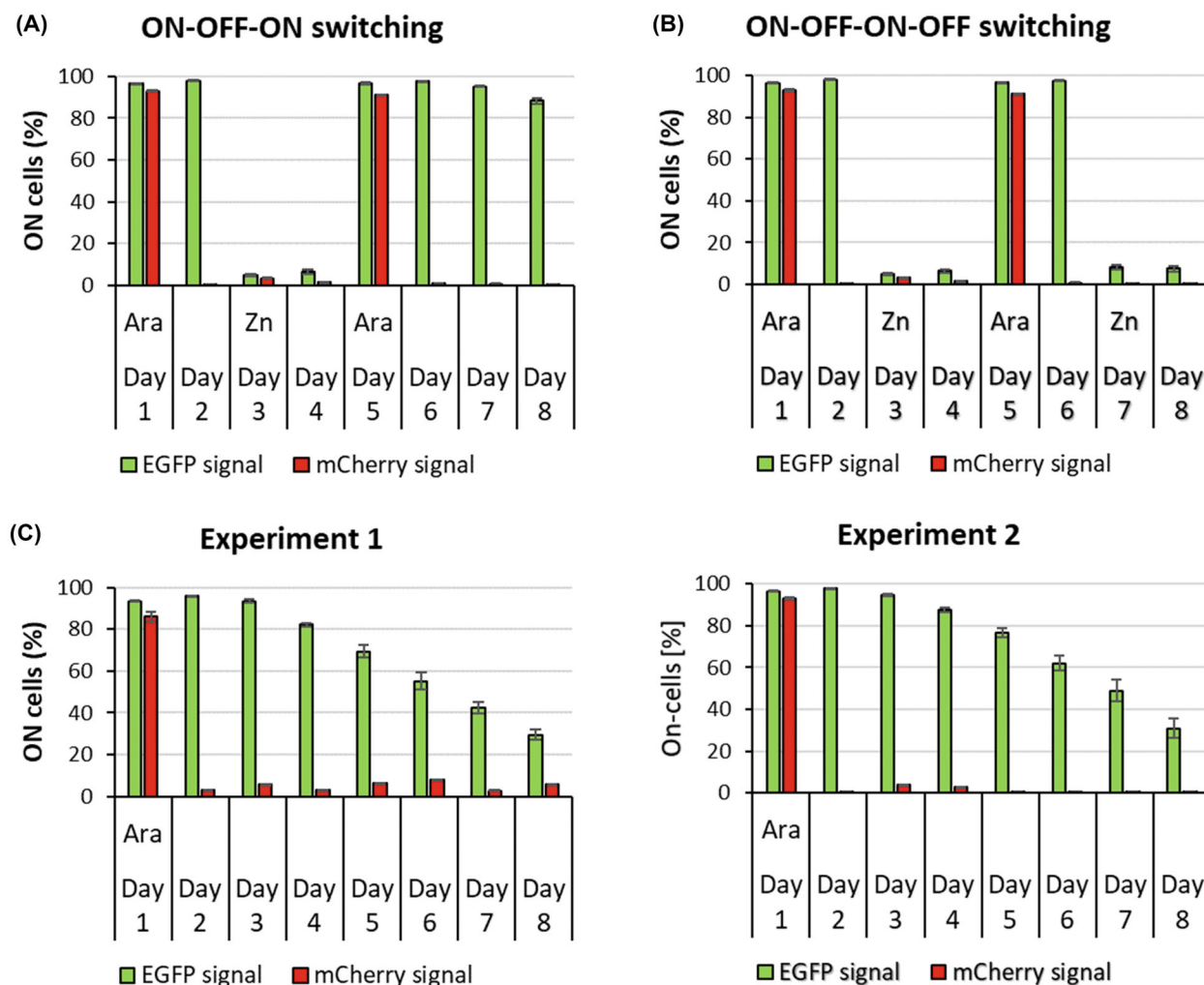


Fig. 2. Flexible switching of the memory system and ON-state stability. (A, B) Flexible ON and OFF switching of the memory system in an ON-OFF-ON (panel A) or ON-OFF-ON-OFF (panel B) switching scheme. (C) Exemplary experiments to study the long-term stability of the ON-state and memory effect of the system. The figure shows the fraction of cells in ON-state represented by the eGFP (green) and mCherry (red) fluorescence signal of the memory and trigger systems. ON- and OFF switching was induced by the addition of arabinose (0.02%, w/v) (indicated by "Ara") and ZnSO₄ (300 μM, indicated by "Zn") to the growth medium. The panels show averages of three independent experiments. The error bar displays the SEM. Primary flow cytometry histograms are shown in Figs S3–S5.

As mentioned in the last paragraph, two (not mutually exclusive) mechanisms could explain the increased activity of ZnF4 at elevated concentrations of ZnSO₄: An increased Zn²⁺-ion concentration could either stabilize the fold of the ZnF4 leading to stronger DNA binding, or it could lead to higher cellular concentrations of ZnF4, because stably folded ZnF4 is more resistant to protein degradation. To investigate this question, the cellular concentrations of ZnF4 were analysed by western blot in cells cultivated at normal (10 μM) or elevated (300 μM) concentrations of ZnSO₄. As shown in Fig. 3D, the increase in ZnSO₄ led to a slight, about 1.5-fold, gain in the cellular concentrations of ZnF4. This

result is in very good quantitative agreement with the increase in ZnF4 target site association by a factor of 1.3 obtained in the modelling, suggesting that this increase in association rate is primarily caused by an increase in the intracellular ZnF4 concentration.

Long-term stability of the ON-state of the memory system

Previous work showed that the ON-state of the memory system is not perfectly stable [12,15,17]. To investigate the mechanism of spontaneous OFF switching of the memory system in more detail, we have studied the

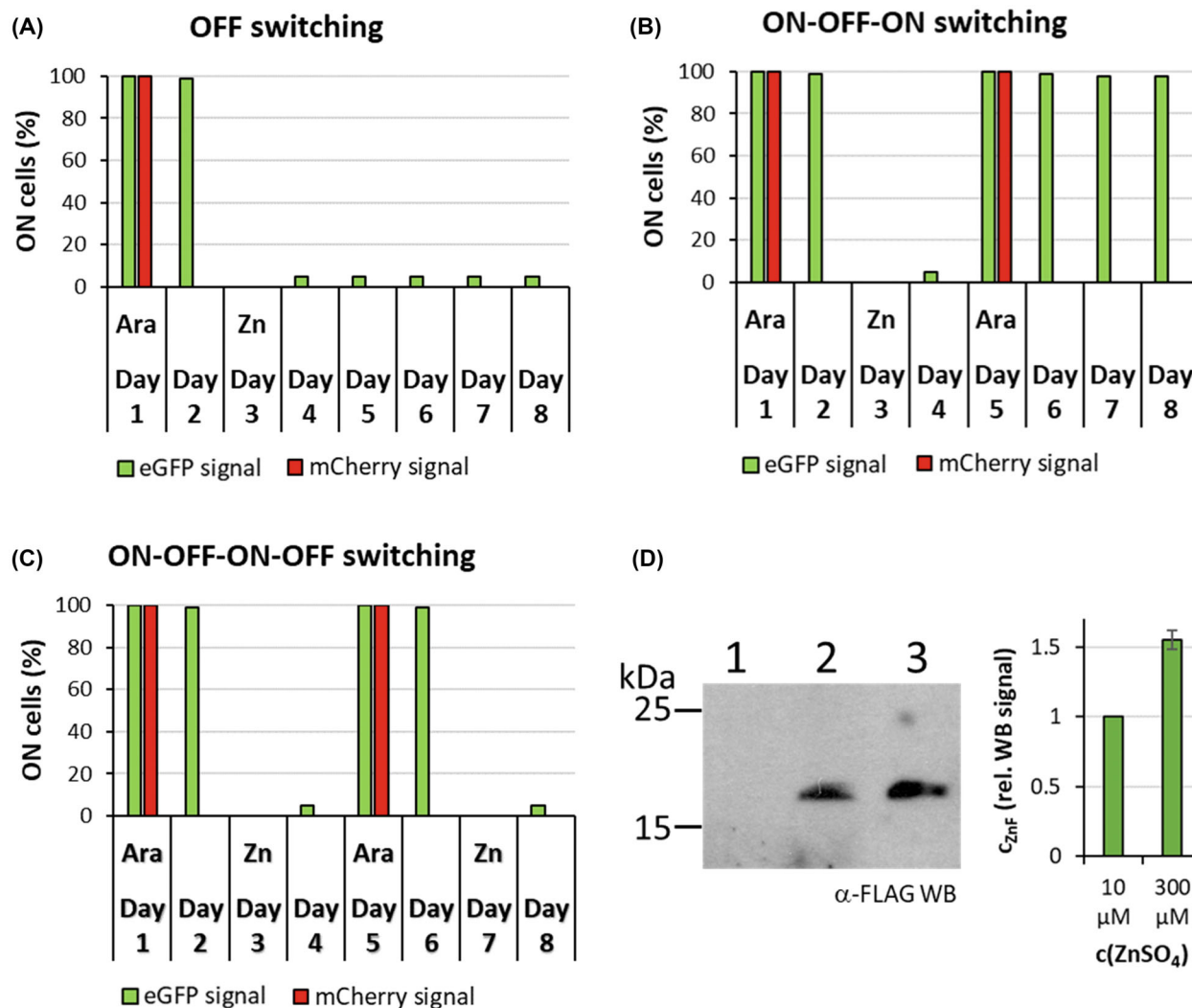


Fig. 3. Modelling of the OFF switching and flexible switching of the memory system. (A–C) Modelling of the ON–OFF (panel A), ON–OFF–ON (panel B) and ON–OFF–ON–OFF (panel C) switching of the system. The corresponding experimental data are shown in Figs 1E and 2A, B respectively. For the simulations, we used the differential equation model described in [17] with parameters as indicated in the Materials and methods section. To mimic population heterogeneity and to simulate the fraction of cells in the ON-state, we used a normal distribution $N(2 \text{ h}, 0.2 \text{ h})$ for the parameter c_c , the cell cycle rate. (D) Western blot analysis of the cellular concentration of the FLAG-tagged ZnF4 in different growth conditions without the addition of arabinose. 1 – untransformed XL1-Blue *Escherichia coli* cells not containing ZnF4, 2 – cells cultivated in medium containing $10 \mu\text{M}$ ZnSO₄ and 0.2% (w/v) D-glucose, and 3 – cells cultivated in medium containing $300 \mu\text{M}$ ZnSO₄ and 0.2% (w/v) D-glucose. The corresponding loading control is shown in Fig. S6. The bar diagram shows the results of a quantitative analysis of two independent experiments. The error bar displays the maximal deviation.

long-term stability of the ON-state. To this end, we analysed the levels of eGFP expression in bacterial ON cultures for up to 200 h, corresponding to roughly 100 cell divisions by flow cytometry at single-cell resolution (Fig. 2C; Fig. S5). In addition, mCherry expression was measured which indicates the transient activity of the trigger system. As shown in previous work, the trigger system was efficiently turned ON after the addition of arabinose to the culture medium, but it was switched OFF already after 1 day of incubation under normal

cultivation conditions. In contrast, eGFP expression was high and almost stable for up to 4 days. In the flow cytometry profiles starting at day 5, a shoulder in the cell population appeared that corresponds to OFF-state cells and the size of this fraction of the population grew over the following days (Fig. 2C; Fig. S5). This observation clearly showed that a biphasic distribution was established in the bacterial culture after some days, which consists of cells which are still in ON-state and cells which have switched into the OFF-state. This

finding indicates that the loss of ON-state signal was caused by individual cells stochastically switching from ON- to OFF-state and not by a drift of the eGFP expression of the entire bacterial population. This result agrees with the predictions from the model, because the positive feedback loop enforces a binary switching of cells between two states [17]. Interestingly, this property of the artificial memory system mimics the behaviour of natural epigenetic switches in bacteria [20,21]. The memory effect of the system is illustrated by the finding that even on day 9 of the experiment, corresponding to roughly 110 cell divisions, a shoulder of ON cells was still detectable (Fig. S5).

DNA methylation analysis in the ON- and OFF-state

To confirm that the observed eGFP expression changes are caused by DNA methylation changes in the ZnF4-binding sites, a DNA methylation analysis at the ZnF4 binding sites was conducted. For this, plasmid DNA was isolated and cleaved with *HinfI* at GANTC sites. DNA cleavage by *HinfI* is inhibited by CcrM methylation and, therefore, the fraction of *HinfI* protection indicated the degree of methylation. The protection level of the amplicon against *HinfI* digestion was determined by qPCR and used to derive the methylation levels assuming an equal distribution of methylation among all ZnF4-binding and CcrM methylation sites. In this analysis, it was considered that the amplicon spans two *HinfI* sites and each site is protected from cleavage if it is in hemi- or fully methylated state, i.e. if one or both DNA strands carry a methylation mark (Fig. 4A). As shown in Fig. 4B, the methylation levels of induced ON-state cultures were around 80%. Interestingly, methylation started to drop even after 1 day of culture when changes in the *egfp* gene expression were not yet detectable. OFF-state cultures were found to contain methylation levels of approximately 5–10% (Fig. 4C), which are not leading to a noticeable inhibition of ZnF4 binding to its binding sites. To define the connection between the declining memory effect of the system and DNA methylation levels, the DNA methylation of an ON-state culture was determined over several days (Fig. 4D) revealing a continuous decline. This result indicates that the drift of cells from the ON- to OFF-state is preceded by a gradual reduction in DNA methylation.

Discussion

In previous work, we established a DNA methylation-based memory system in bacteria that responds to an arabinose trigger by a switch into an ON-state leading to

persistent eGFP expression [12]. However, available data showed that the ON-state of the memory system is not perfectly stable [12,15,17]. Moreover, a system reset so far could only be realized by including an additional orthogonal system to control the proteolytic digestion of the CcrM DNA methyltransferase [12] which has limited applicability. Both of these issues are related to insufficient control of the OFF switching of the system, which leads to signal loss if it occurs spontaneously, but could also be used for system reset if induced intentionally.

In this work, these two processes for switching the DNA methylation-based memory system from the ON- into the OFF-state have been investigated: (a) the enforced OFF switch by chemical treatment and (b) the spontaneous switch of dividing bacterial cells from the ON- into the OFF-state. Regarding the first question, we show that increasing the ZnSO₄ concentration of the bacterial cultivation media leads to a small but significant 1.5-fold increase in the ZnF4 concentration, which is sufficient to trigger the switch of the memory system from the ON- into OFF-state, which was then stable over several days even at normal ZnSO₄ concentrations. These observations are consistent with the results of a steady-state analysis of our computational model [17], which indicated that stability of the ON-state is completely lost by a small 1.3-fold increase in the ZnF4 DNA association rate, resulting in a fast switch of the system back to the OFF-state upon an increase in ZnSO₄. Afterwards, the OFF-state was stable, even at normal concentrations of ZnSO₄.

In contrast, the ON-state was not stable after the removal of arabinose and, starting at day 5, part of the cellular population switched back into the OFF-state (Fig. 3C). We were interested to understand the molecular mechanism behind this OFF switching and therefore tried to describe the time dependence of the fraction of cells in the ON-state mathematically. Our first assumption was that a simple monomolecular kinetic model could describe the OFF-switching effect. In this model, each ON-state cell at each time point has a fixed probability to switch into the OFF-state. However, as shown by the blue lines in Fig. 5A, this model could not at all recapitulate the data. Therefore, we next devised a model, in which the probability of OFF switching of an ON-state cell (P_{OFF}) is zero immediately after the ON switch, but it increases linearly by a fixed increment (ΔP) with each cell division (N).

$$P_{\text{OFF}}(N) = \Delta P \times N.$$

Strikingly, as shown by the grey lines in Fig. 5A, this model described the data very accurately with ΔP values of $3.1 (\pm 0.2) \times 10^{-4}$, although it contains only

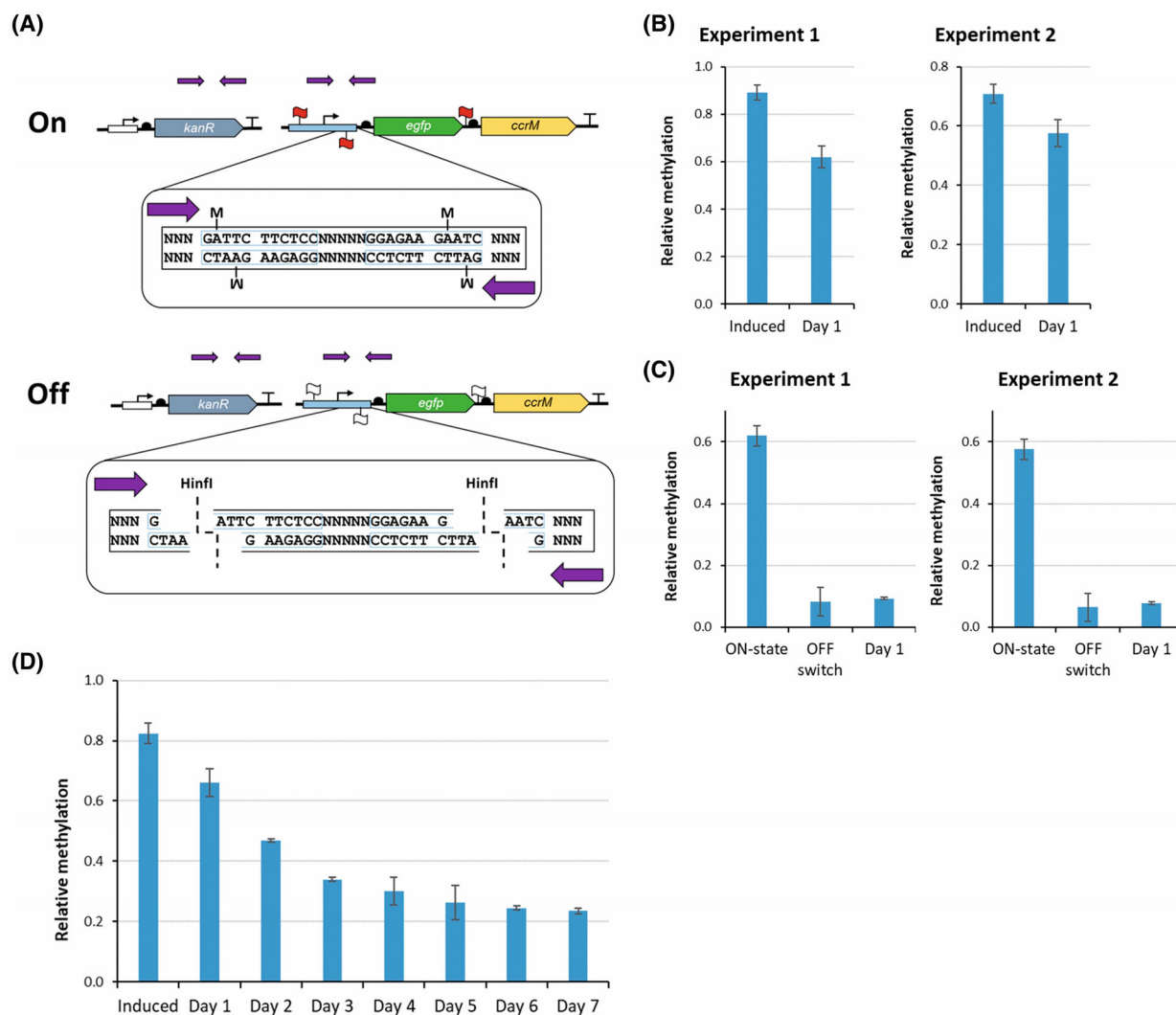


Fig. 4. DNA methylation analysis of ON- and OFF-state cells. (A) Experimental design of the qPCR methylation analysis. In the ON-state, CcrM target sites are predominantly methylated. In this state, the CcrM-sensitive restriction enzyme *Hinfi* is not able to cut the target regions. In the OFF-state, *Hinfi* cleaves the target region used as a template for qPCR due to the absence of methylation. Internal normalization of the input DNA amount was performed by amplification over a region not affected by *Hinfi*. Red and white flags symbolize methylated and unmethylated palindromic ZnF4-binding sites. (B) Methylation levels in ON-state. (C) Methylation levels during the switch from ON- to OFF-state. (D) Long-term methylation analysis of ON cultures. Shown are relative methylation levels derived from the qPCR data. Data show averages of three independent experiments, error bars display the SEM.

one variable parameter (ΔP). This result indicates that the memory effect of the system is very strong immediately after the ON switch, but it is slowly declining with each cell division.

Our methylation data showed that the DNA methylation at the ZnF4-binding sites that is introduced during the ON switch gradually decreases and apparently the decline in methylation preceded the OFF switching. This finding suggests that the reduction in DNA methylation is responsible for the declining memory effect described in the previous paragraph. To connect

these two processes more accurately, we first assumed that ZnF dimers connected by a coiled-coil bind to a palindromic zinc finger-binding site (ZFBS) in a cooperative manner. The palindromic ZFBS contains two adenine residues, one in each DNA strand, that are relevant for ZnF binding (Fig. 1B). Therefore, the fractions of unmethylated, hemimethylated and fully methylated palindromic ZFBS were calculated which is corresponding to the experimentally determined average methylation levels assuming a random distribution of the methylation. The ZFBS methylation states were

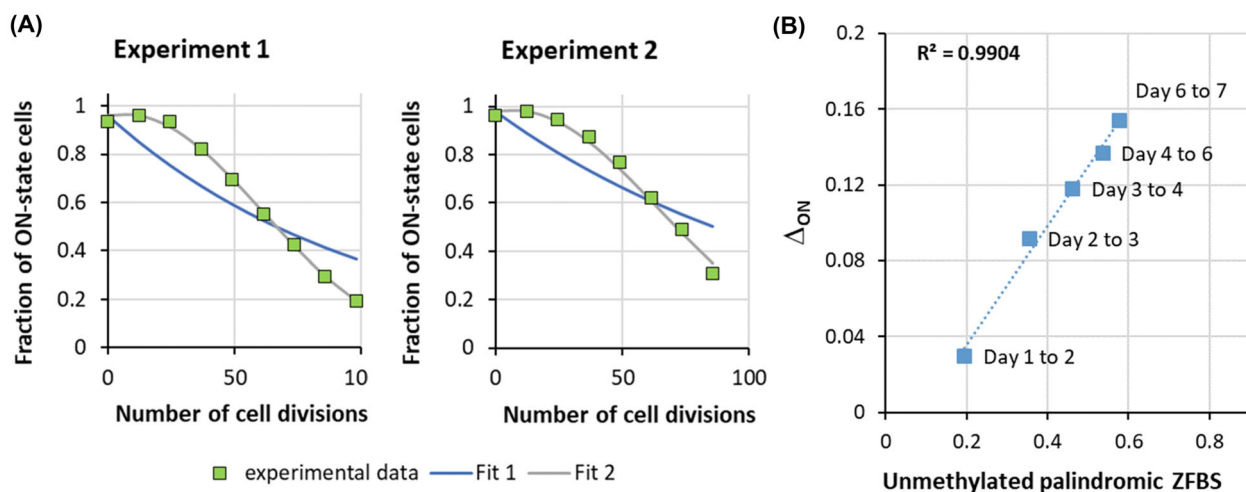


Fig. 5. Analysis of the long-term stability and methylation of the ON-state. (A) Quantitative analysis of the experimental data of the long-term stability of the ON-state shown in Fig. 2C. Shown are experimental data (green squares) and fits to a monomolecular kinetics (Fit 1, blue curves) and to a memory decay reaction (Fit 2, grey curves). Values obtained for ΔP were 3.32×10^{-4} per cell division for experiment 1 and 2.93×10^{-4} per cell division for experiment 2. (B) Correlation of the loss of ON cells (Δ_{ON}) and the fraction of unmethylated palindromic ZnF4 binding sites. The loss of ON cells, $\Delta_{ON} = ON(\text{day}_N) - ON(\text{day}_{N+1})$, was taken from panel A. The average fraction of unmethylated palindromic ZFBS at day_N and day_{N+1} was derived from the data shown in Fig. 4D.

then correlated with the experimentally determined average loss of ON-state cells in Fig. 5A from 1 day to the next (Δ_{ON}). Strikingly, Δ_{ON} was very strongly correlated with the fraction of unmethylated palindromic ZFBS with an R^2 of 0.99 (Fig. 5B). As a next step, we considered that two ZnF dimers of ZnF4 bind to two palindromic ZFBS. Therefore, the fractions of all combinations of methylation states of the two palindromic ZFBS were calculated as well. However, the correlations with the other more complex methylation patterns were always weaker than the correlation with the appearance of single unmethylated palindromic ZFBS. This result suggests that it is the appearance of individual, unmethylated palindromic ZFBS, which triggers OFF switching and causes the loss of the memory effect by allowing an enhanced binding of the ZnF4 protein to this binding site.

In conclusion, the data described above lead to the following scenario describing the spontaneous OFF switching of ON-state cells: We determined that bacterial cells contain approximately 150 copies of the memory plasmid under our experimental conditions, which are highly methylated at the ZnF4-binding sites in the ON-state leading to low ZnF4-binding affinity. After DNA replication, the sites are converted into the hemimethylated state which corresponds to a loss of 50% of their methylation and leads to an increased (but still relatively low) ZnF4 binding. At this point, ZnF4 and CcrM compete for access to the unmethylated sites. If CcrM gets access, the site will be methylated and

further ZnF4 binding will be inhibited. Conversely, bound ZnF4 can temporarily prevent re-methylation and also stop transcription of the memory *ccrM* gene in this plasmid. Hence, transient ZnF4 binding leads to a small reduction in CcrM pool of the cells. This, however, leads to less efficient CcrM competition with ZnF4, initiating a slow drift of reduction in cellular CcrM content. The slow reduction in CcrM concentration causes a similar reduction in methylation levels of ZnF4-binding sites, as observed in our experiments. If CcrM concentration has fallen below a certain threshold value, the residual amount of CcrM is no longer able to remethylate the ZnF4-binding sites leading to a switch of the corresponding cell into the OFF-state. The continuously ongoing weak reduction in average CcrM concentration in the cells explains the reduction in the memory effect in the system, where the probability of switching from the ON- into the OFF-state increases with the number of cell divisions after the initial trigger event. The artificial switch by increased $ZnSO_4$ concentrations enforces this process, because higher concentrations of ZnF4 lead to more efficient DNA binding and repression of *ccrM* transcription.

Conclusions

We show here that efficient OFF switching of the memory system can be achieved by adding an external small molecule component into the growth medium. Based on this, we demonstrate that bacterial cultures

can be switched between the ON- and OFF-state in an easy and reversible manner, illustrating the capacity of the bacterial memory system for reversible information storage. Moreover, our new insights into the mechanism of ON-state instability will support future design to further stabilize the ON-state and enforce the binary behaviour of the system. One conceivable approach could be to increase the memory CcrM concentration, for example, by using a stronger promoter or placing two *ccrM* genes in the operon.

Materials and methods

Bacterial cultivation and regulated ON and OFF switching of the memory system

Cultivation of *E. coli* XL1-Blue cells containing the bacterial memory system components was conducted as described [15,19] in LB medium supplemented with 0.2% (w/v) D-glucose, antibiotics and 10 μM ZnSO_4 . Due to the low thermostability of ZnF4, which caused spontaneous induction of the system at higher temperatures as previously observed [12], cultivation was carried out at 28 °C. The switching between ON- and OFF-states at specific time points was regulated by changing to the ON-state trigger media (25 $\mu\text{g}\cdot\text{mL}^{-1}$ kanamycin, 100 $\mu\text{g}\cdot\text{mL}^{-1}$ ampicillin, 10 μM ZnSO_4 and 0.02% (w/v) arabinose) or OFF-state trigger medium (25 $\mu\text{g}\cdot\text{mL}^{-1}$ kanamycin, 100 $\mu\text{g}\cdot\text{mL}^{-1}$ ampicillin, 300 μM ZnSO_4 and 0.2% (w/v) D-glucose) for 24 h. Afterwards, the cells were diluted 1 : 50 000 in a normal growth medium.

Determination of the plasmid number of the memory plasmid

To determine the number of memory plasmids in each cell, XL1-Blue *E. coli* cells transfected with trigger and memory plasmid were cultivated as described above. Upon an OD_{600} of ~ 0.9 , plasmid isolation was performed from 1 mL cell culture using the NucleoSpin® Plasmid purification kit (Macherey-Nagel GmbH & Co. KG, Düren, Germany). Five-hundred nanogram of the sample was digested with 20 U PvuII-HF (New England Biolabs, Frankfurt am Main, Germany) for 2 h at 37 °C, which leads to a specific digestion profile for trigger and memory plasmid. Afterwards, the digested sample was separated on 1% agarose gels, and the intensities of the obtained signals corresponding to memory or trigger plasmid were analysed using IMAGEJ [22]. Considering the ratio between memory and trigger plasmid and the OD_{260} of the DNA preparations, the concentration of memory and trigger plasmid in each sample was calculated. With the concentration of the memory plasmid and the given molar mass and total volume of the DNA sample, the molar concentration was converted into the molecule

number. Assuming that 1 OD_{600} corresponds to 8×10^8 cells $\cdot\text{mL}^{-1}$ (<https://www.labtools.us/bacterial-cell-number-od600/>), the number of memory plasmid numbers per cell was derived.

Flow cytometry analysis

The detection of the reporter gene expression was carried out by flow cytometry as previously described [15]. In short, cells were cultivated up to an OD_{600} of ~ 1.2 . Samples of 300 μL were taken and centrifuged at 11 000 g for 3 min. The cell pellet was washed with 1.5 mL Z-buffer (60 mM Na_2HPO_4 , 40 mM NaH_2PO_4 , 10 mM KCl and 1 mM MgSO_4 , pH 7) and fixed with 1% PFA (Paraformaldehyde EM Grade, 00380-1; Polysciences Europe GmbH, Hirschberg an der Bergstraße, Germany, in Z-buffer). The fixed cells were centrifuged again at 11 000 g for 3 min, resuspended in 600 μL Z-buffer and filtered through 30 μL Pre-Separation Filters (Miltenyi Biotec, Bergisch Gladbach, Germany). Flow cytometry data were evaluated with the FLOWJO v10.8.0 software (FlowJo BD, Heidelberg Germany). Gates were optimized by comparing the single-cell population for eGFP and mCherry fluorescent area in normalized histograms as shown in Fig. S1. Flow cytometry histograms of all experiments are shown in Figs S2–S5.

Methylation analysis

Methylation at the palindromic ZnF4-binding sites was analysed by the protection of HinfI cleavage as described [12] using a qPCR amplicon that contains two HinfI cleavage sites. If both sites are hemi- or fully methylated, the amplicon is protected from cleavage, leading to a complex relationship between methylation and protection levels as described [17]. The reaction was carried out with biological and technical replicates and analysed by qPCR using the CFX96 Connect Real-Time System (Bio-Rad Laboratories GmbH, Feldkirchen, Germany) together with the ORA™ SEE qPCR Green ROX L Mix (highQu GmbH, Kraichtal, Germany).

Analysis of zinc finger levels in the ON- and OFF-states

To analyse the FLAG-tagged ZnF4 expressed from the memory plasmid in the bacterial cultures under low and high ZnSO_4 conditions, western blot experiments were conducted. For this, 3 mL of cultures cultivated in LB medium supplemented with 100 $\mu\text{g}\cdot\text{mL}^{-1}$ ampicillin, 25 $\mu\text{g}\cdot\text{mL}^{-1}$ kanamycin, 0.2% (w/v) D-glucose and 10 or 300 μM ZnSO_4 with an OD_{600} of 0.9 were harvested and centrifuged at 4500 g for 8 min. The cell pellet was resuspended in 100 μL GST-Sonication buffer (50 mM Tris-HCl pH 7.5, 150 mM NaCl, 1 mM DTT and 5% glycerol) together with 1 μL of

Protease Inhibitor Cocktail (13.5 mM bestatin, 13.4 mM leupeptin, 9.3 mM E-64, 6 mM pepstatin A, 0.25 mM aprotinin and 0.12 mM AEBSF•HCL). Cell lysis by sonication was performed using the EpiShear™ Probe Sonicator (Active Motif Europe, Waterloo, Belgium). Each sample was sonicated five times for 20 s with an amplitude of 20% and a pause phase of 30 s between every sonication step. Thereafter, the cell lysate was centrifuged at 13 000 *g* for 10 min at 4 °C. Two microlitre of supernatant was separated by 16% SDS-gel electrophoresis and afterwards transferred onto a nitrocellulose membrane (Amersham™ Protan™ 0.2 μm NC; GE Healthcare Europe, Freiburg, Germany). For loading control, the membrane was incubated for 15 min in Ponceau S solution (0.2% Ponceau S and 3% trichloroacetic acid) at RT and an image was taken (Fig. S6). For the detection of the FLAG-tagged ZnF4 protein, a monoclonal Anti-Flag M2 antibody (Sigma-Aldrich Chemie GmbH, Taufkirchen, Germany; Lot: SLBQ6349V, 1 : 1000) and as a secondary antibody Anti-mouse IgG HRP (GE Healthcare Europe; Lot: 17246087, 1 : 5000) were used.

Determination of bacterial growth curves

The growth kinetics of the *E. coli* cultures in the ON- and OFF-states were determined in standard cultivation medium by measuring the optical density (OD₆₀₀) every hour (Fig. S7). Fits of the initial parts of the data to exponential growth curves revealed growth rates (μ) of 0.38 h⁻¹ for OFF-state cells and 0.39 h⁻¹ for ON-state cells.

Mathematical modelling

For the modelling, we adopted the model described in Klingel [17], which was built to describe the induction of the memory system by different trigger inputs and fitted to time-course data of eGFP and mCherry signals and methylation levels. This model comprises four state variables which correspond to the fraction of binding sites not bound by ZnF4 (variable x_1), the fraction of methylated methylation sites (variable x_2), relative amounts of maintenance and trigger CcrM (variables x_3 and x_4 , respectively), as quantified by eGFP and mCherry signals. The normalized model reads:

$$\dot{x}_1 = c_c(1-x_1) + d_1(1-x_1)p^{x_2} - u_1(t)a_1x_1,$$

$$\dot{x}_2 = a_2x_1(1-x_2)(rx_3 + x_4) - c_cx_2,$$

$$\dot{x}_3 = \frac{k_3}{r}x_1 - d_cx_3,$$

$$\dot{x}_4 = k_4u_2(t) - d_cx_4.$$

It uses the following inputs:

$$u_1(t) = \begin{cases} u_1^m & t = T_{Zn} \\ 1 & \text{else} \end{cases}$$

and

$$u_2(t) = \begin{cases} u_2^m & t = T_{Ara} \\ 1 & \text{else} \end{cases}$$

with T_{Ara} and T_{Zn} corresponding to the cultivation phase with trigger media for the ON- or OFF-state with arabinose or ZnSO₄ respectively.

Parameter values were copied from [17] with the addition of $u_{1,m}$ for the OFF switch and are given below:

$\hat{\theta}_i$	a_1	a_2	d_1	d_c	p	k_3	k_4	r	$u_{1,m}$	$u_{2,m}$
Log($\hat{\theta}_i$)	1.25	0.37	-0.85	-0.3	1.72	1.04	-0.8	-0.99	1.3	1.11

Simulation of cell populations was done by assuming a normal distribution $N(2 \text{ h}, (0.2 \text{ h})^2)$ for the cell cycle rate c_c . Model trajectories were simulated by integration of the ODE model with independent samples from this normal distribution. Simulations were conducted in MATLAB R2020a (MathWorks, Natick, MA, USA) using the IQM-Toolbox. This enables the use of the CVODE solver from SUNDIALS for the conversion and simulation of the model in C.

Acknowledgements

Funded by the Deutsche Forschungsgemeinschaft DFG JE 252/35-1 (AJ) and DFG NR 1840/2-1 (NER) and under Germany's Excellence Strategy – EXC 2075 – 390740016 (NER and AJ) is gratefully acknowledged. Open Access funding enabled and organized by Projekt DEAL.

Conflict of interest

The authors declare no conflict of interest.

Author contributions

AJ, SW and NER devised the work. DG and LL performed the experiments. AJ and SW supervised the biochemical work. All authors were involved in data analysis and interpretation. VK performed the modelling and supervised by NER. AJ, DG and SW prepared the draft of the manuscript with input from all authors. All authors approved the final version of the manuscript.

Peer review

The peer review history for this article is available at <https://publons.com/publon/10.1111/febs.16690>.

Data availability statement

All data are included in this work and its [Supporting Information](#). Source data are available from the corresponding author upon reasonable request.

References

- Slomovic S, Pardee K, Collins JJ. Synthetic biology devices for in vitro and in vivo diagnostics. *Proc Natl Acad Sci USA*. 2015;**112**:14429–35.
- Chang HJ, Voyvodic PL, Zuniga A, Bonnet J. Microbially derived biosensors for diagnosis, monitoring and epidemiology. *J Microbial Biotechnol*. 2017;**10**:1031–5.
- Hicks M, Bachmann TT, Wang B. Synthetic biology enables programmable cell-based biosensors. *ChemPhysChem*. 2020;**21**:132–44.
- Del Valle I, Fulk EM, Kalvapalle P, Silberg JJ, Masiello CA, Stadler LB. Translating new synthetic biology advances for biosensing into the earth and environmental sciences. *Front Microbiol*. 2020;**11**:618373.
- Lloyd JPB, Ly F, Gong P, Pflueger J, Swain T, Pflueger C, et al. Synthetic memory circuits for stable cell reprogramming in plants. *Nat Biotechnol*. 2022. <https://doi.org/10.1038/s41587-022-01383-2>
- Bashor CJ, Collins JJ. Understanding biological regulation through synthetic biology. *Annu Rev Biophys*. 2018;**47**:399–423.
- Feinberg AP. Phenotypic plasticity and the epigenetics of human disease. *Nature*. 2007;**447**:433–40.
- Wion D, Casadesus J. N6-methyl-adenine: an epigenetic signal for DNA-protein interactions. *Nat Rev Microbiol*. 2006;**4**:183–92.
- Schubeler D. Function and information content of DNA methylation. *Nature*. 2015;**517**:321–6.
- Allis CD, Jenuwein T. The molecular hallmarks of epigenetic control. *Nat Rev Genet*. 2016;**17**:487–500.
- Sanchez-Romero MA, Cota I, Casadesus J. DNA methylation in bacteria: from the methyl group to the methylome. *Curr Opin Microbiol*. 2015;**25**:9–16.
- Maier JAH, Möhrle R, Jeltsch A. Design of synthetic epigenetic circuits featuring memory effects and reversible switching based on DNA methylation. *Nat Commun*. 2017;**8**:15336.
- Olivenza DR, Nicoloff H, Sanchez-Romero MA, Cota I, Andersson DI, Casadesus J. A portable epigenetic switch for bistable gene expression in bacteria. *Sci Rep*. 2019;**9**:11261.
- Park M, Patel N, Keung AJ, Khalil AS. Engineering epigenetic regulation using synthetic read-write modules. *Cell*. 2019;**176**:227–38.e20.
- Ullrich T, Weirich S, Jeltsch A. Development of an epigenetic tetracycline sensor system based on DNA methylation. *PLoS One*. 2020;**15**:e0232701.
- Maier JAH, Jeltsch A. Design and application of 6mA-specific zinc-finger proteins for the readout of DNA methylation. *Methods Mol Biol*. 2018;**1867**:29–41.
- Klingel V, Kirch J, Ullrich T, Weirich S, Jeltsch A, Radde NE. Model-based robustness and bistability analysis for methylation-based, epigenetic memory systems. *FEBS J*. 2021;**288**:5692–707.
- Studier FW. Protein production by auto-induction in high density shaking cultures. *Protein Expr Purif*. 2005;**41**:207–34.
- Klingel V, Graf D, Weirich S, Jeltsch A, Radde NE. Model-based design of a synthetic oscillator based on an epigenetic methylation memory system. *ACS Synth Biol*. 2022;**11**:2445–55.
- Garcia-Pastor L, Sanchez-Romero MA, Jakomin M, Puerta-Fernandez E, Casadesus J. Regulation of bistability in the std fimbrial operon of *Salmonella enterica* by DNA adenine methylation and transcription factors HdfR, StdE and StdF. *Nucleic Acids Res*. 2019;**47**:7929–41.
- Sanchez-Romero MA, Olivenza DR, Gutierrez G, Casadesus J. Contribution of DNA adenine methylation to gene expression heterogeneity in *Salmonella enterica*. *Nucleic Acids Res*. 2020;**48**:11857–67.
- Schneider CA, Rasband WS, Eliceiri KW. NIH Image to IMAGEJ: 25 years of image analysis. *Nat Methods*. 2012;**9**:671–5.

Supporting information

Additional supporting information may be found online in the Supporting Information section at the end of the article.

Fig. S1. Gating strategy used for cell sorting.

Fig. S2. Exemplary flow cytometry histograms of the experiments to study the long-term stability of the OFF-state after ON–OFF switching shown in Fig. 1E.

Fig. S3. Flow cytometry histograms of the experiments to study the flexible ON–OFF–ON switching of the system shown in Fig. 2B.

Fig. S4. Flow cytometry histograms of the experiments to study the flexible ON–OFF–ON–OFF switching of the system shown in Fig. 2C.

Fig. S5. Flow cytometry histograms of the experiments to study the long-term stability of the ON-state and memory effect shown in Fig. 2A.

Fig. S6. Loading control of the western blot analysis of the cellular concentration of ZnF shown in Fig. 3D.

Fig. S7. Bacterial growth kinetics of in ON- and OFF-states.